SUSAN SALHIA
IRC-LIBRARY
AECL
2251 SPEAKMAN DR
MISSISSAUGA, ON L5K 1B2
CANADA

ORDER NUMBER:	**CI-04886638-2**
Account Number:	FGH24244
Delivery Mode:	FTP
Delivery Address:	
Submitted:	2004/08/19 09:24:03
Received:	2004/08/19 09:24:03
Printed:	2004/08/19 12:09:22

Direct	**Conference**	**WWW Catalogue**	**CANADA**
12			
$ 12.00			

Client Number:	ROBERT ION - SP/0479
Title:	**8TH ANNUAL CONFERENCE 1987 : 16-17 JUNE 1987, SAINT JOHN, NEW BRUNSWICK, CANADA : PROCEEDINGS**
Author:	CANADIAN NUCLEAR SOCIETY. CONFERENCE (8TH : 1987 : SAINT JOHN, N.B.)
DB Ref. No.:	IRN13925647
Date:	1987
Pages:	125 - 134
Article Title:	REGIME-4 CODE FOR PREDICTION OF FLOW REGIME TRANSITION IN A HORIZONTAL PIPE, ANNULUS, AND BUNDLE FLOW UNDER GAS-LIQUID TWO-PHASE FLOW,
Article Author:	S.I. OSAMUSALI AND J. S. CHANG
Report Number:	IRN13925647
Publisher:	THE SOCIETY,
Information Source:	INNOPAC

Estimated cost for this 10 page document: $11.4 document supply fee + $0 copyright = $11.4

REGIME -4 CODE FOR PREDICTION OF FLOW REGIME TRANSITION IN A HORIZONTAL PIPE, ANNULUS AND BUNDLE FLOW UNDER GAS-LIQUID TWO-PHASE FLOW

S.I. OSAMUSALI AND JEN-SHIH CHANG
Dept. of Engineering Physics, McMaster University
Hamilton, Ontario, Canada L8S 4M1

ABSTRACT

REGIME-4 code for prediction of flow regime transition in a horizontal pipe, annulus and bundle geometries under cocurrent gas-liquid two-phase flow has been developed, and an experimental confirmation has been conducted. The results show that the present code predicts relatively well all flow regime transitions for these geometries.

INTRODUCTION

The ability to predict the transition locations between the various flow patterns occurring in a two phase flow system is important for the determination of the heat and mass transfer rates, as well as the flow pressure drop of the system. In nuclear power plants, this information is also useful for modelling postulated Loss of Coolant Accidents (LOCA). For the cocurrent pipe flow, extensive research has been conducted and there now exist some acceptable mechanistic models capable of predicting the approximate locations of these transition boundaries. However, it has not been well established whether these pipe flow models can be applicable to the annulus and rod bundle geometries.

Earlier investigations on the rod bundle geometry include Bergles and Roos[3], Williams and Peterson[4], Aly[5], Nicholson et al.[6], Chang et al.[13], Krishnan and Kowalski[7] and Venkateswararao[8]. These were mostly experimental, using probe methods for flow regime characterization. Venkatessararao[8] and Minato et al.[9], also studied the vertical 24-rod and horizontal 37-rod bundle geometries theoretically, respectively.

In this work, the mechanistic approach of Taitel and Dukler[1] are modified to account for the effect of surface tension force in the Helmholtz instability model for the stratified to intermittent transition criteria. This is then extended to modelling horizontal rod bundle geometries where the geometrical effect of each individual rod present is well accounted. Experimental studies have also been conducted for an air-water two phase flow system at room temperature and at atmospheric pressure.

FLOW REGIME

As in single-phase fluid mechanics, various 'flow regimes' are found to exist in a two-phase flow system. However, unlike single-phase systems where the regimes are basically restricted to two structures, laminar and turbulent, two-phase systems are capable of producing a much wider range of flow patterns. These regimes result from the particular manner in which the two phases are distributed in the pipe.

Though authors define each flow regime somewhat differently, most agree that there are six basic structures. Examples of these flows are shown in figure 1. In this study the flow regime analysis will be based on the definitions below.

Stratified smooth flow (SS) occurs when the liquid is flowing at the bottom of the pipe and the gas flows along the top. The surface of the liquid is smooth. Stratified wavy flow (SW) is similar to stratified smooth, however, the gas-liquid interface is wavy. Both elongated bubble (this is designated as plug (PL) flow) and slug (SL) flow are what Taitel and Dukler[1] call intermittent (I) flow and are characterized by the liquid bridging the gap between the gas-liquid interface and the top of the pipe. The difference between slug and plug flow depends on the degree of agitation of the bridge. This work follows the definition of Taitel and Dukler. Plug flow is considered to be the limiting case of slug flow where no entrained bubbles exist in the liquid slug.

Annular flow (A) occurs when the walls are wetted by a thin film of liquid while the gas, at high velocity, flows through the centre of the pipe. Liquid droplets are usually entrained in this gas. When the upper walls are periodically wetted by large aerated waves it is neither slug flow, which requires a complete fluid bridge, nor annular flow, which requires a stable film. Taitel and Dukler[1] designated this flow pattern as wavy annular flow. However, this regime was not recognized by Mandhane et al.[2] and was considered to be slug flow.

In the dispersed bubble (DB) or bubbly regime small gas bubbles are distributed throughout the liquid phase which otherwise completely fills the pipe. The transition to this regime is characterized by the gas bubbles losing contact with the top of the tube. At first, the bubbles are near the upper portion of the pipe but at higher liquid flow rates become uniformly distributed throughout the system.

In the model presented in this study, the process of analyzing the transitions between flow regimes starts from the condition of stratified flow. An equilibrium stratified flow is assumed and the mechanism whereby a change from stratified flow can be expected to take place is imposed on the system. The condition of stratified smooth flow being central to this analysis, it is first necessary to develop a generalized relationship for stratified flows.

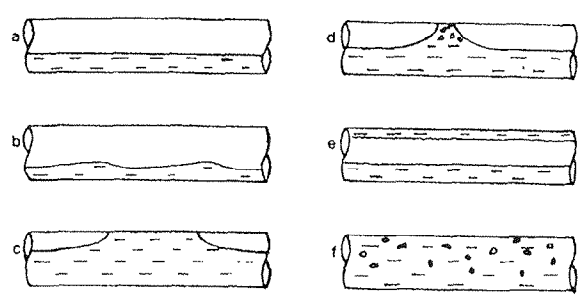

Fig.1 Flow Regime Structures.
Flow Regimes in Horizontal Two-Phase Flow
a) Stratified Smooth b) Stratified Wavy
c) Plug d) Slug e) Annular f) Dispersed Bubble

Equilibrium Stratified Flow (One-Dimensional)

The situation assumed in this analysis is shown in figure 2, where g and ℓ represent the gas and liquid phases, respectively. The flow is assumed to be non-accelerating and stratified smooth. Here, the method of Taitel and Dukler[1] is used to analyze the flow. A simple momentum balance on each phase (figure 2) assuming no pressure differential across the fluid-fluid interface yields

$$-\frac{dP}{dz} - \tau_\ell \frac{S_\ell}{A_\ell} + \tau_i \frac{S_i}{A_\ell} = 0 \qquad (1)$$

and

$$-\frac{dP}{dz} - \tau_g \frac{S_g}{A_g} - \tau_i \frac{S_i}{A_g} = 0 \qquad (2)$$

In the above equations the interfacial shear has opposite signs for each phase in accordance with Newton's third law. Subtracting these two equations we obtain

$$-\tau_\ell \frac{S_\ell}{A_\ell} + \tau_g \frac{S_g}{A_g} + \tau_i S_i \left(\frac{1}{A_\ell} + \frac{1}{A_g} \right) = 0 \qquad (3)$$

The shear stresses are evaluated in the conventional manner using the form suggested by Blasius[10],

$$\tau_\ell = f_\ell \rho_\ell \frac{u_\ell^2}{2}; \quad \tau_g = f_g \rho_g \frac{u_g^2}{2}; \quad \tau_i = f_i \rho_g \frac{(u_g - u_i)^2}{2} \qquad (4)$$

with the friction factors evaluated from

$$f_\ell = C_\ell \left(\rho_\ell \frac{D_\ell u_\ell}{\mu_\ell} \right)^{-x_\ell}; \qquad f_g = C_g \left(\rho_g \frac{D_g u_g}{\mu_g} \right)^{-x_g} \qquad (5)$$

The hydraulic diameters in the above equations are evaluated in the usual way as four times the fluid area divided by the 'wetted' perimeter. However, in this case, the method of Agrawal et al.[11] is followed where it is assumed that the wall resistance is similar to that of open channel flow for the liquid and closed channel flow for the gas. Analysis indicates however, that changes in this assumption have little effect on the outcome. The resulting expressions for the hydraulic diameters are

$$D_\ell = 4 \frac{A_\ell}{S_\ell}; \qquad D_g = \frac{4A_g}{S_g + S_i} \qquad (6)$$

To determine an expression for the interfacial friction factor we assume $f_i = f_g$ in accordance with the results of Gazely[12] and $u_g >> u_i$. These are verified a posteriori by direct comparison with experimental results.

In the evaluation of the constants in the Blasius equation it is assumed that the results from single-phase analysis may be applied directly. For the case of steady laminar flow the variables C and x are 16.0 and 1.0, respectively, corresponding to Poiseuille flow. For steady turbulent flow, these parameters have the values 0.046 and 0.2, respectively, corresponding to the well known Blasius equation for smooth pipe flow. In this analysis the transition to turbulent motion is assumed to occur in a given phase when the fluid's Reynolds number, given by the terms in brackets in equation 5 exceeds 2000. Here, again, the possible effect of surface waves is ignored.

Equations 3 to 6 fully describe the two-phase stratified flow once the expressions for the geometrical parameters of the system are obtained. Simple analysis of figure 2 yields the following expressions for the pipe geometry

$$A_\ell = \frac{D^2}{4} \left[\pi - \arccos(\gamma) + \gamma \sqrt{1-\gamma^2} \right] \qquad (7)$$

$$A_g = \frac{\pi D^2}{4} - A_\ell \qquad (8)$$

$$S_\ell = D[\pi - \arccos(\gamma)] \qquad (9)$$

$$S_g = \pi D - S_\ell \qquad (10)$$

$$S_i = D\sqrt{1-\gamma^2} \qquad (11)$$

where

$$\gamma = 2h_\ell/D - 1 \qquad (12)$$

For the general case of the annulus geometry with the rod located at position R(r,θ),the following expressions for the geometric parameters are obtained for the three regions of the equilibrium liquid level, h_ℓ, as shown in Figure (3)

(i)

$$h_\ell \le \left[\frac{1}{2}(D-d) + r\,Sin\theta \right]$$

$$A_\ell' = A_\ell \qquad (13)$$

$$A_g' = A_g - \frac{\pi d^2}{4} \qquad (14)$$

$$S_\ell' = S_\ell \qquad (15)$$

$$S_g' = S_g + \pi d \qquad (16)$$

$$S_i' = S_i \qquad (17)$$

(ii)

$$\left[\frac{1}{2}(D-d) + r\,Sin\theta \right] < h_\ell < \left[\frac{1}{2}(D+d) + r\,Sin\theta \right]$$

$$A_\ell' = A_\ell - \frac{d^2}{4} \left[\pi - \arccos(\beta) + \beta \sqrt{1-\beta^2} \right] \qquad (18)$$

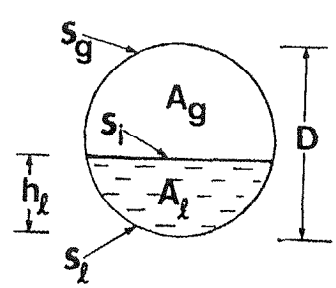

Fig. 2 Equilibrium Stratified Horizontal Pipe Flow.

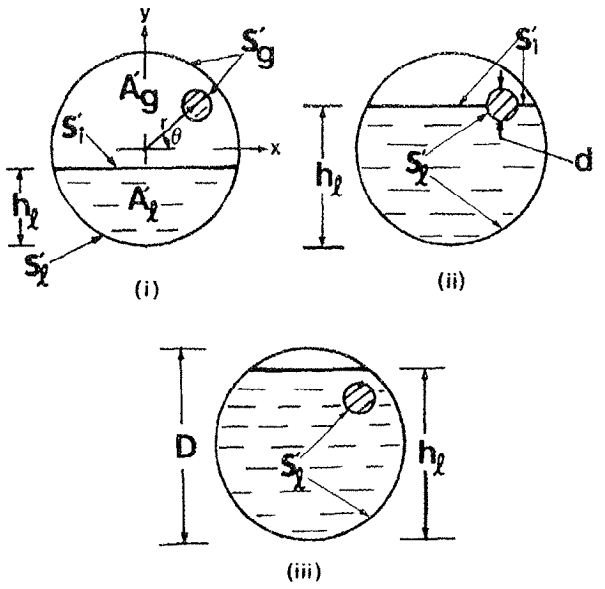

Fig. 3 Equilibrium Stratified Horizontal Annulus Geometry Flow for Different Cases of the Liquid Level.

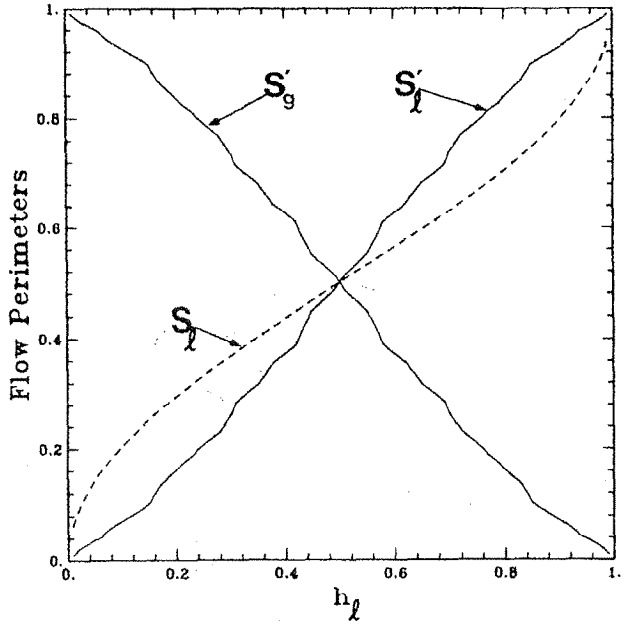

Fig. 4 Calculated Liquid Perimeter, S_ℓ, and Gas Perimeter, S_g, for the 37-Rod Bundle.

$$A'_g = \frac{\pi}{4}(D^2 - d^2) - A'_\ell \tag{19}$$

$$S'_\ell = S_\ell + d\left|\pi - \arccos(\beta)\right| \tag{20}$$

$$S'_g = \pi(D+d) - S'_\ell \tag{21}$$

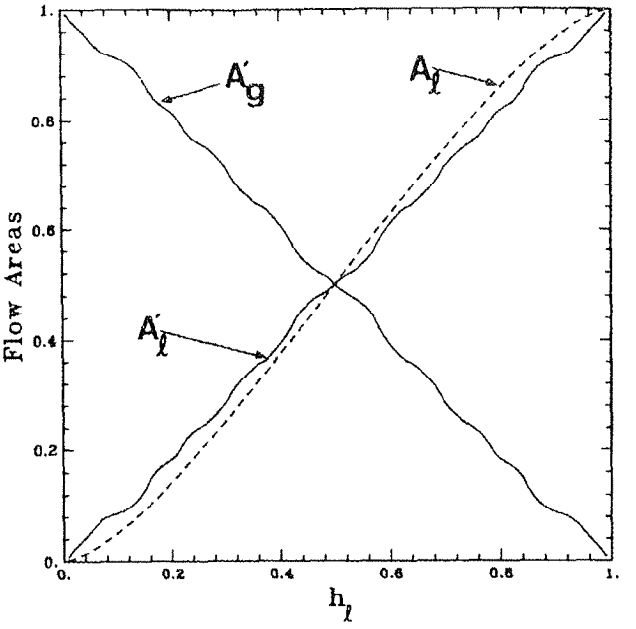

Fig. 5 Calculated Liquid Area, A_ℓ, and Gas Area, A_g, for the 37-Rod Bundle.

$$S'_i = S_i - d\sqrt{1-\beta^2} \tag{22}$$

where

$$\beta = (2h_\ell - D - 2r\,\mathrm{Sin}\theta)/d$$

(iii)

$$h_\ell \geq \left|\frac{1}{2}(D+d) + r\,\mathrm{Sin}\theta\right|$$

$$A'_\ell = A_\ell - \frac{\pi d^2}{4} \tag{23}$$

$$A'_g = A_g \tag{24}$$

$$S'_\ell = S_\ell + \pi d \tag{25}$$

$$S'_g = S_g \tag{26}$$

$$S'_i = S_i \tag{27}$$

The special case for the concentric annular geometry corresponds to the rod being at location R(0,0)[13]. In the above expressions for the annulus geometry, we have simply subtracted the contributions to A_ℓ, A_g, and S_i due to the presence of the rod from those given in equations (7), (8) and (11) for the enclosing pipe geometry and added the contributions to S_ℓ and S_g to those given in equations (9) and (10).

The values of these geometric parameters for the rod bundle case can simply be obtained by computing the above expressions for every rod in the system located at position $R_i(r_i, \theta_i)$.

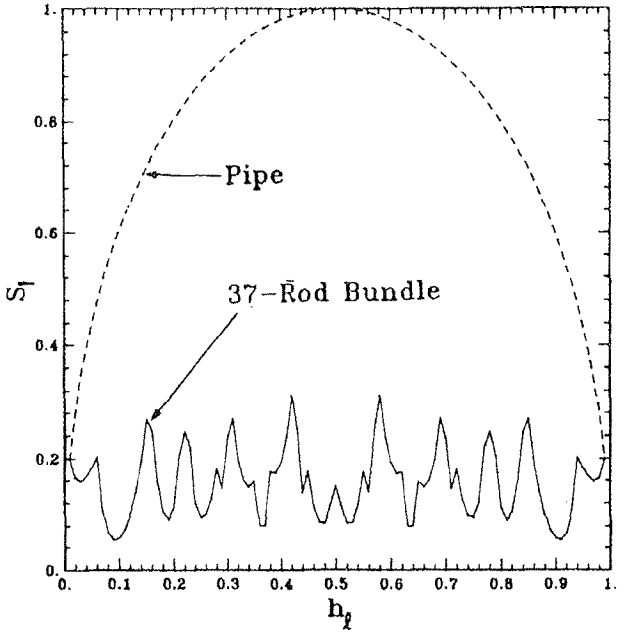

Fig. 6 Calculated Interfacial Length, S_i, for the 37-Rod Bundle.

Typical calculations of the geometric parameters for 37-rod bundle case are shown in Figures (4) to (6), where the geometric parameter for the tube are also compared with present results in Figures 4 to 6. Figures 4 to 6 show that the parameters such as S_g, S_ℓ and S_i are significantly influenced by existence of the bundles while little influence for A_g and A_ℓ is observed. Figure 6 also shows that the interfacial area becomes nonmonotonic in the case of bundle geometries, and order of magnitude small compared with tube cases.

Transition Criteria

(i) Transition to Intermittent or Annular Flow. The essential mechanism for transition from stratified to intermittent flows is the unconfined growth of a surface wave instability. For a 'critical' set of flow conditions a wave travelling on a stratified surface will grow until the wave blocks the flow of the gas phase. At low gas flow rates the blockage forms a complete (though possibly agitated) bridge and plug or slug flow results. At higher gas flow rates there may be insufficient liquid flowing to properly sustain the 'bridge'. As a result the liquid in the wave is swept up around the inner wall of the pipe resulting in annular flow. The growth of a wave may take place owing either to a) the action of the gas flowing over it or b) due to the action of surface tension which 'pulls' the liquid up to form the complete bridge. Neglecting the motion of the fluids, the conditions for wave growth may be written, for the first case as[14]:

$$u_g > 1.414\, B \left[\frac{g(\rho_\ell - \rho_g) A_g}{\rho_g \dfrac{dA_\ell}{dh_\ell}} \right]^{1/2} \tag{28}$$

$$B = 1 - \frac{h_\ell}{D} \tag{29}$$

The above expression for B, due to Taitel and Dukle[1], corresponds closely to the results obtained from previous analysis of the same problem by Wallis and Dobson [15] and Kordyban and Ranov[16]. These analyses, like the model of Taitel and Dukler, propose that the transition to intermittent flow depends on the value of B. In this study a criterion of B = 0.5 is taken as the condition which distinguishes intermittent from annular or wavy annular flow. For B greater than 0.5 the flow is considered annular, for B less than 0.5 the flow is intermittent.

The term dA_ℓ/dh_ℓ appearing in equation 28 may be determined directly from differentiation of A_ℓ for the pipe or A_ℓ' for the annulus and rod bundle cases, respectively.

For pipes of small diameter, surface tension may have important effects on the flow regime structure. A wetting liquid has a tendency to climb the inner tube wall due to a capillary force. As a result of this force, the climbing liquid forms a complete bridge and intermittent flow ensues.

The transition to plug flow at low gas and liquid flow rates is modelled by comparing the gravity and surface tension forces.

Ignoring the motion of both fluids, the transition criteria is given by[24]:

$$h_g \leq \frac{\pi}{4} \left[\frac{\sigma}{\rho g \left(1 - \frac{\pi}{4}\right)} \right]^{1/2} \tag{30}$$

For pipe sizes smaller than a certain maximum equation 30 is always satisfied. In these cases, transition will take place whenever the liquid level will be high enough to satisfy mass balance.

Transition to Stratified Wavy Flow. For the case of a steady state two-phase flow, the formation of a stratified wavy structure is associated with the situation where the velocity of the gas is sufficient to cause waves to form (through interfacial shear) but slower than that needed to cause transition to intermittent flow. For the 'non-accelerating' case the work of Jeffreys[17] is introduced. He postulated the following condition for wave generation.

$$c(u_g - c)^2 > \frac{4\mu_\ell g(\rho_\ell - \rho_g)}{\rho_\ell \rho_g s} \tag{31}$$

In the above inequality s is a sheltering coefficient. Jeffreys suggested a value of s = 0.3 while other researchers[1,18] have recommended much smaller values of the order of s = 0.01. Clearly the value of s depends on how one defines a wave. A variety of different wave structures on two-phase stratified surfaces have been described[19]. They may be listed in three main groups; ripple waves, two dimensional waves and three dimensional waves. In this report the value of s = 0.01 is used.

The constant c which appears in equation 31 is the speed of the waves. For most cases of importance, it is assumed that $u_g >> c$. Previous theories and experimental results[20,21,22] indicate that the ratio of wave velocity to mean liquid film velocity decreases with increasing liquid Reynolds number. For turbulent flow this ratio is near 1.0. Thus for simplicity the relation of $u_\ell = c$ is used.

Substituting the above approximations into equation 31 the criterion for transition from stratified smooth to stratified wavy flow becomes

$$u_g \geq \left[\frac{4g\mu_\ell(\rho_\ell - \rho_g)}{s\rho_\ell \rho_g u_\ell} \right]^{1/2} \tag{32}$$

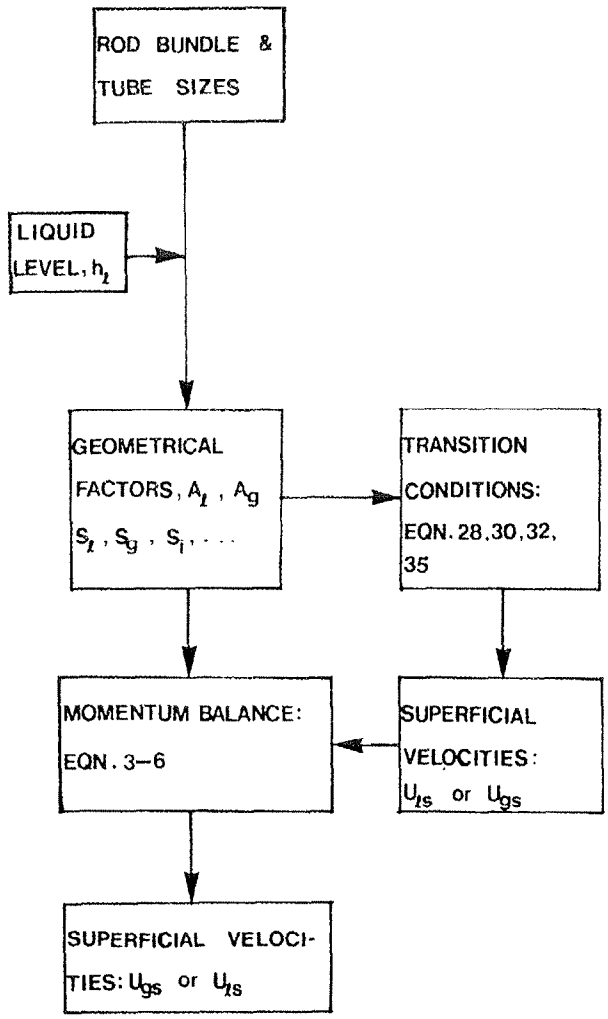

Fig. 7 Schematic Flowchart of the REGIME-4 Code.

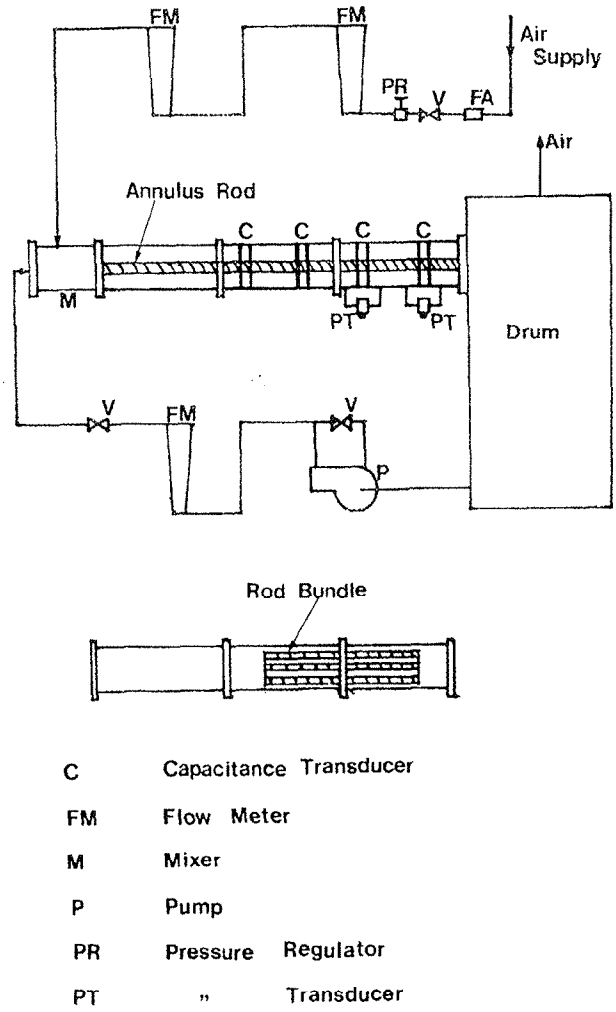

Fig. 8 Schematic Diagram of Experimental Loop.

Transition to Dispersed Bubble Flow. In intermittent flow, the elongated gas bubbles formed are observed to flow on top of the liquid duc to buoyancy effects. However, at higher liquid flow rates than those encountered in intermittent flow, the gas phase tends to mix with the fast flowing liquid leading to dispersed gas bubbles in the liquid phase. This occurs when the turbulent fluctuations overcome the buoyancy forces[1]. The buoyancy force per unit length of the gas region is

$$F_B = g(\rho_\ell - \rho_g) A_g \tag{33}$$

and the turbulent force acting on the gas is

$$F_T = \frac{1}{4} S_i \rho_\ell f_\ell u_\ell^2 \tag{34}$$

Therefore, the condition for transition to dispersed bubble flow regime as stated earlier, namely, $F_T \geq F_B$ becomes

$$u_\ell \geq \left[\frac{4\, g(\rho_\ell - \rho_g) A_g}{f_\ell \rho_\ell S_i} \right]^{1/2} \tag{35}$$

For transitions in annulus and rod bundle geometries, the appropriate geometric parameters for these cases are used in the transition criteria given by equations 28, 29, 32 and 35.

NUMERICAL PROCEDURE

The theoretical transition boundaries discussed above are calculated numerically by program REGIME-4. The procedure used in REGIME-4 is shown in the flow charts of figure 6.

LOOP DESCRIPTION AND EXPERIMENTAL PROCEDURE

A schematic diagram of the experimental loop is as shown in Figure 7. This.is a recirculating air-water system having a transparent section made of acrylic tubing 5.08 cm I.D. and 365.76 cm long. Water is pumped from a large separator tank through a rotameter (Fischer and Porter Co. type) calibrated up to a maximum flow rate of 1.11 [ℓ/s]. Air from the laboratory supply is flowed past a pressure regulator, an air filter and through a rotameter (Brooks Instruments type, Model #1110-10H3A1D) calibrated up to a maximum flow rate of 11.33 [ℓ/s]. The air and water flow through a separated type mixing section into the test section.

The redistribution of the two phases within the test section for different flow rates of air and water are monitored with the analogue output signals of the ring-type capacitance transducers[23] via a Boonton capacitance meter, Model No. 72B.

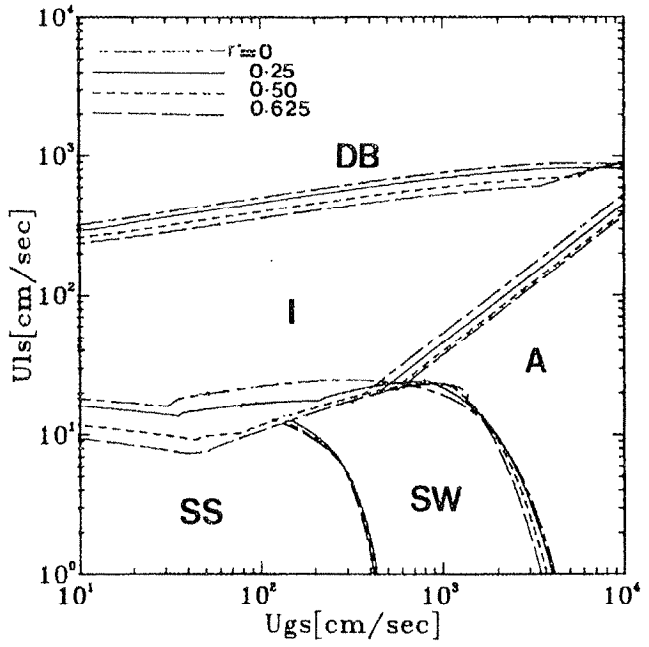

Fig. 9 Calculated Annulus Geometry Flow Regime Map for Different Diameter Ratios.

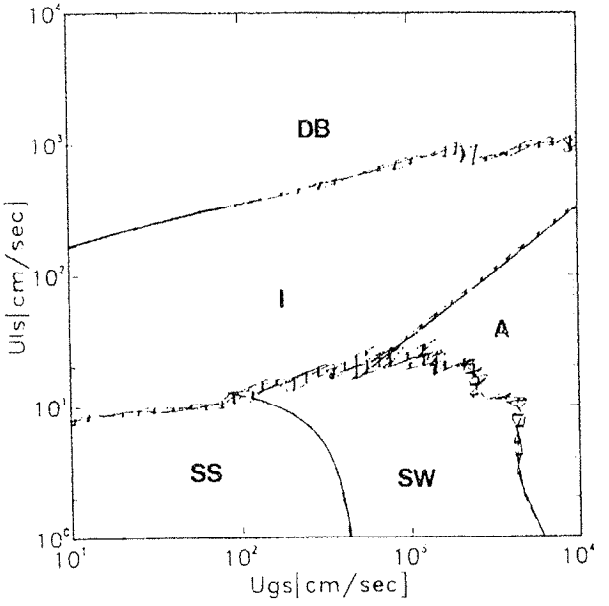

Fig. 10 Calculated 37-Rod Bundle Flow Regime Maps for Different Rotation Angles.

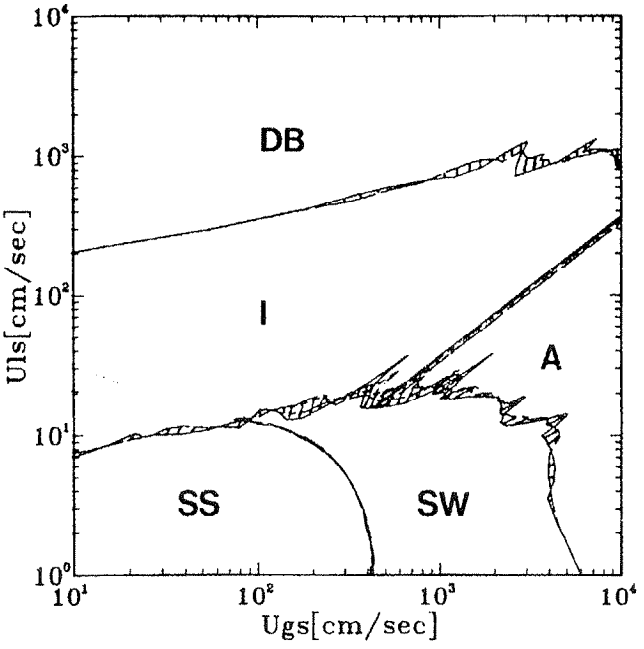

Fig. 11 Calculated 28-Rod Bundle Flow Regime Maps for Different Rotation Angles.

For the annulus geometry, a rod is placed along the central axis of the pipe and the two-phase flow regime characterization repeated as in the case of the pipe.

This present loop is slightly modified to accomodate two 37-rod bundles, 100.00 [cm] long, placed next to each other in the downstream of the test section. A 10.16 [cm] I.D. tubeshell is used in the test section of the loop. This is constructed out of two 150.00 [cm] long sections of clear anodized aluminum materials and a 150.00 cm long transparent section of acrylic material placed in the downstream of the test section. A homogeneous type mixing section design is used in this case. The two-phase flow regime characterizations are accomplished using analogue output signals of the ring-type capacitance transducers.

NUMERICAL RESULTS

Figure (9) shows the numerical results for the annulus geometry where different ratios of the rod to pipe internal diameter in the range of 0.250 to 0.625 have been considered. The internal diameter of the tubeshell considered is 5.08 [cm]. This is presented in the form of a flow regime map based on the liquid and gas superficial velocities. Figure (10) shows the flow regime maps for the 37-rod bundle geometry for different rotation angles from 0° to 45°. The flow regime map for the 28-rod bundle is also presented in Figure (11).

DISCUSSIONS

Pipe Flow

Figure (12) illustrates the effect of including surface tension forces in the Hemholtz instability criteria for transition from stratified to intermittent or annular flow regimes for the 5.08 [cm] I.D. pipe. The results for larger line sizes of up to 20.00 [cm] I.D. have been given by Lightstone et al.[14] who found the flow regime transitions to vary strongly with diameter.

Annulus

The numerical results for the concentric annulus of figure (9) shows that the flow regime transitions are significantly influenced by tube diameter ratios, and are also different from those of the normal pipe flow. The stratified to intermittent or annular transitions were the most affected. This can be likened to the dependence of flow regimes on pipe diameters as has been observed by Lightstone et al.[14]. The flow regime transitions for the annulus of diameter ratio, r = 0.25,

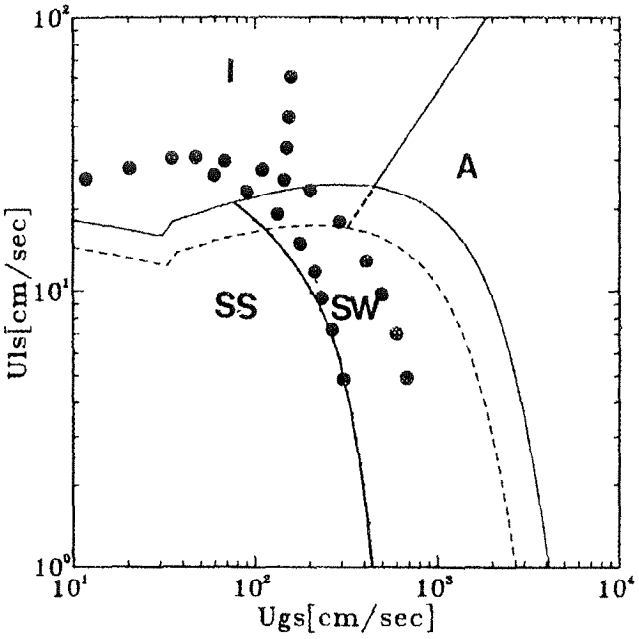

Fig. 12 Flow Regime Maps for the 5.08 [cm] I.D. Pipe With and Without Accounting for Surface Tension Forces.

• • • Experiment
– – – – Taitel & Dukler
——— This Work

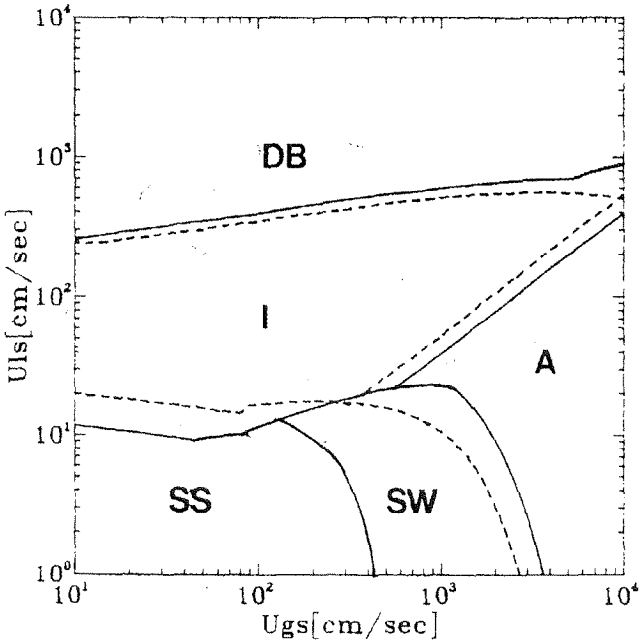

Fig. 13 Calculated Results for Annulus of Diameter Ratio, $r^* = 0.50$ and Pipe of Equivalent Diameter, $D_{equ} = 2.540$ [cm].

——— Annulus
– – – – – Equiv. Pipe

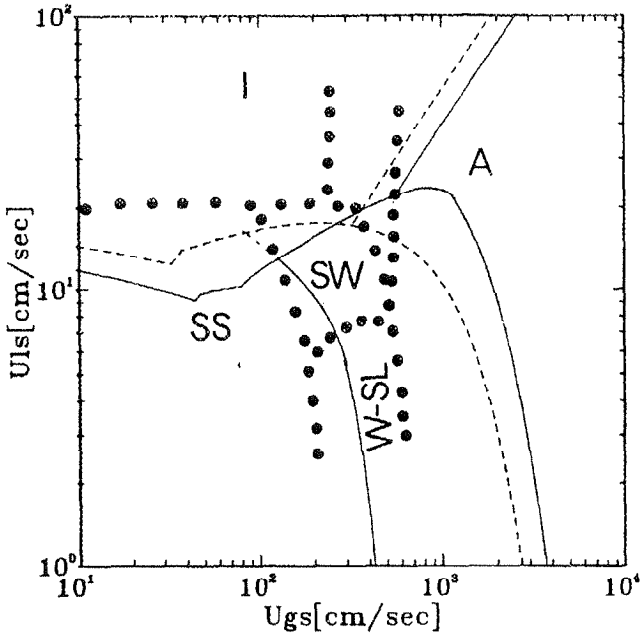

Fig. 14 The Experimental and Theoretical Results of the Annulus Geometry with Diameter Ratio of 0.5.

• • • Experiment
——— Annulus
– – – 5.08 cm Pipe

which corresponds to an equivalent pipe diameter of 0.75D is closer to those of the pipe than with larger diameter ratios, r = 0.500 and r = 0.625. Figure (13) shows that the intermittent region for the annulus is larger than that for a pipe of equivalent diameter. Nicholson et al.[25] observed opposite trend experimentally with the annulus for an air-oil two-phase flow system. Nicholson et al. suggested that this may be due to the annulus central rod damping out waves that would otherwise grow to form slugs in the tube-flow. In figure (14), the experimental results for the concentric annulus with a diameter ratio of 0.500 is compared with calculated values. Figure (14) also shows the calculated value for the enclosing tubeshell of internal diameter, 5.08 cm I.D. without rod at its central axis. The results of figure (14) show a significant effect of the rod on the flow regime transitions. The stratified to intermittent or annular transition is seen to occur earlier for the concentric annular geometry than the pipe case at low superficial gas velocities. The experimental results show a wavy-slug flow regime which is characterized by the liquid tending to bridge the gap between the gas-liquid interface and the lower surface of the rods. This occurs at low superficial liquid velocities for high superficial gas rates. This soon changes into the annular flow regime at higher gas rates. The discrepancy between the experimental data and theoretical results in the transition between stratified and intermittent or annular flow regimes may be due to the fact that this transition boundary is usually not sharply defined. This may also be due to the fact that the effect of frictional forces has not been considered in the mechanism governing this transition.

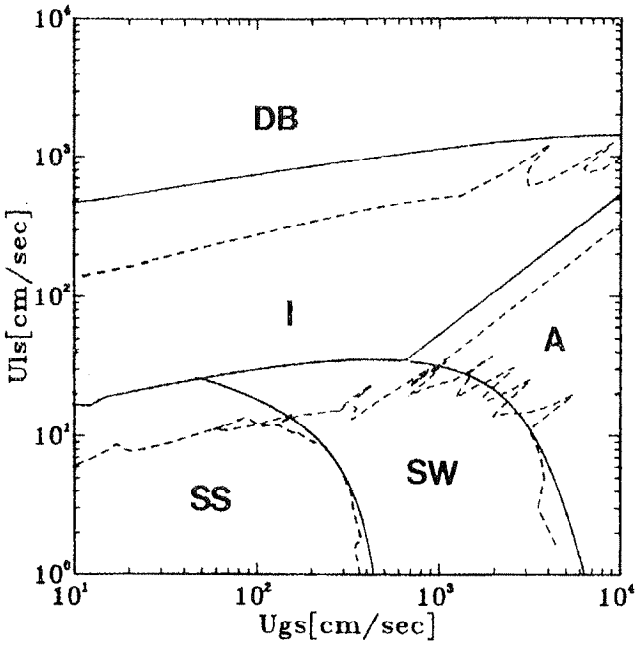

Fig. 15 Comparison of the Calculated 37-Rod Bundle Results and That of a Pipe.

– – – Bundle

——— Pipe (10.34cm I.D)

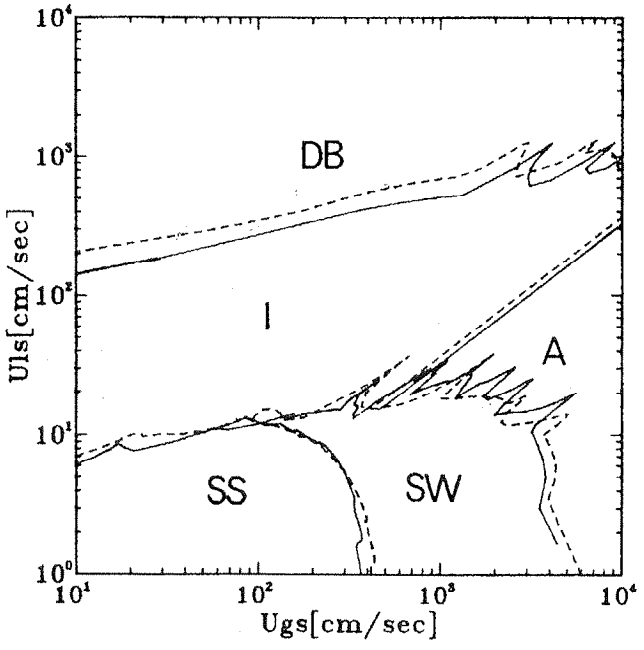

Fig. 16 Comparison of the Calculated Results for 37- and 28-Rod Bundles.

———37, – – – –28

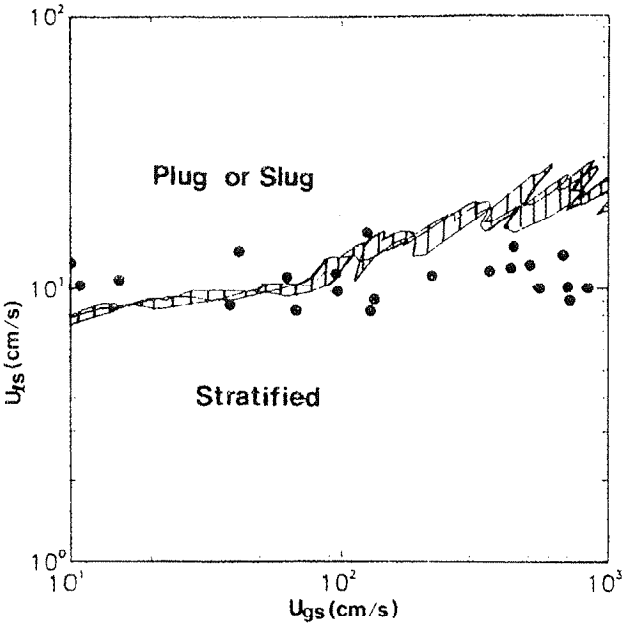

Fig. 17 Comparison of Calculated and Experimental Results for the 37-Rod Bundle.

● ● ● Minato et al.

Rod Bundle

The stratified to intermittent or annular transitions for the 37-rod bundle geometry maps shown in Figure (10) indicate the existence of unstable transition locations at high superficial gas velocities. This may be a complex case of the wavy-slug and wavy-annular flows observed experimentally for the concentric annular geometry. In this case, however, the liquid rate is high enough to bridge the gap between the gas-liquid interface and the top of the enclosing tubeshell sweeping across rows of rods in the bundle. At higher gas flow rates, in the region where transition to annular flow is expected to occur, this liquid bridge is swept around the surface of the rods and the inner surface of the enclosing tubeshell. In the subchannel approach for rod bundles, situations similar to the wavy-slug flow of the annulus case may be identified strictly as slug flow, while the liquid rates may not be high enough to cause transition to slug flow as predicted by this full-channel approach to rod bundle flow regime analysis. Figure (10) also shows that the particular orientation of the 37-rod bundle in the enclosing tubeshell affects flow regime transitions. The 37-rod bundle flow regime map of Figure (12) is for rod bundle orientations of 0° through 45°. The transition boundaries are shown as bands rather than sharp lines. These results account for any orientation of the rod bundle within the enclosing tubeshell.

The results of Figure (15) seem to confirm the predicted effects on flow regime transitions due to the presence of rods in the system as was already discussed for the annulus geometry. However, this variation of the flow regime transitions is enhanced by the increased number of rods in the rod bundle geometry. Figure (16) shows the numerical results for the 37- and 28-rod bundle geometries to be different.

Figure (17) shows a comparison between the calculated and experimental results of Minato et al.[7] for the 37-rod bundle geometry. The results show that the present model predicts not only well the transition boundary, but also agrees with the uncertainty region caused by the orientation of the bundles.

CONCLUSIONS

In this work, the numerical results for flow regimes of the pipe, annulus and rod bundle geometries are presented. These have been confirmed by direct comparison with experiments. The results show that:

(1) For large pipe diameters, surface tension forces become important in the mechanism for transition between stratified and intermittent or annular flow regimes.

(2) The flow regime transitions for the annulus geometry is quite different from those of the pipe.

(3) The wavy-slug flow regime experimentally observed for the annulus occurs at low liquid superficial velocities for high gas rates. This flow structure may become important during the rewetting of nuclear reactor fuel rod bundles.

(4) The flow regime transitions for the rod bundle geometries are quite different from those of the pipe, and also vary with the the rod bundle orientation within the enclosing tubeshell. The transition boundaries for any orientation can be represented by bands. The transition boundaries for the rod bundle geometry also showed the existence of finger-type instability region at high gas flow rates.

Acknowledgement

The authors wish to express their gratitude to M. Shoukri, P.E. Wood, T.G. Beuthe, D. Groenveld and S. Sutradhar for valuable discussions comments. This work was supported partly by the Natural Sciences and Engineering Research Council of Canada.

REFERENCES

(1) TAITEL, Y and DUKLER, A.E., "A Model for Predicting Flow Regime Transitions in a Horizontal and near Horizontal Gas-Liquid Flow", AIChE J., Vol. 22, No. 1, pp. 47-55, 1976.

(2) MANDHANE, J.M., GREGORY, G.A., and AZIZ, K., "A Flow Pattern Map for Gas-Liquid Flow in Horizontal Pipes", Int. J. Multiphase Flow, Vol.1, pp. 537-553, 1974.

(3) BERGLES, A.E. and ROOS, J.P."Investigation of Boiling Flow Regimes and Critical Heat Flux", USAEC, New York Operation Report No. NYO-3304-12, 1968.

(4) WILLIAMS, G.L. and PETERSON, A.C., "Two-Phase Flow Patterns with High Pressure Water in a Heated Four-Rod Bundle", Nucl. Sci. Eng., Vol. 68, No. 2, pp. 155-159, 1981.

(5) ALY, A.M.M., "Flow Regime Boundaries for an Interior Sub-channel of a Horizontal 37-Element Bundle", Can. J. Chem. Eng., Vol. 59, No. 2, pp. 158-163, 1981.

(6) NICHOLSON, M.K. and NICKERSON, J.R., "A Comparison of Flow Regime Behaviour in Adiabatic and Diabatic Two-Phase Trefoil Simulations", Second Int. Tropical Meeting on Nuclear Thermalhydraulics, Santa Barbara, 1983.

(7) KRISHNAN, V.S., and KOWALSKI, J.E., "A Study of the Stratified Slug Flow Transition in a Horizontal Pipe containing a Rod Bundle", AIChE Symposium Series, Vol. 80, No. 236, pp. 282-289, 1984.

(8) VENKATESWARARAO, P., SEMIAT. R., and DUKLER, A.E., "Flow Pattern Transition for Gas-Liquid Flow in a Vertical Rod Bundle", Int. J. Multiphase Flow, Vol. 8, No. 5, pp. 509-524, 1982.

(9) MINATO, A. IKEDA, T. and NAITOH, M., Private Communications, 1986.

(10) BLASIUS, H. "Das Ahnlichkeitsgesetz bei Reibungsuorgangen in Flussigkeiten", Forschg. Arb. Ing.-Wes., No. 134, 1913.

(11) AGRAWAL, S.S., GREGORY, G.A. and GOVIER, G.W., "An Analysis of Horizontal Stratified Two-Phase Flow in Pipe", Can J. Chem. Eng., vol. 51, pp. 280-286, 1973.

(12) GAZELY, C., "Interfacial Shear and Stability in Two-Phase Flow", Ph.D. Thesis, Univ. Delaware, Newark, 1949.

(13) CHANG, J.S., REVANKER, S.T., RAMAN, R., and TRAN, F.B.P., "Application of an EHD Technique to a Nuclear Power Plant Emergency Core Cooling System", IEEE Trans. Industrial Appl. Vol. IA-21, No. 4, pp. 715-723, 1985.

(14) LIGHTSTONE, L., OSAMUSALI, S.I. and CHANG, J.S., "REGIME-3 Code for Prediction of Flow Regime Transition in a Two-Phase Manifold Flow", 13th Annual Can. Nucl. Soc. Simulation Symposium, April, 1987.

(15) WALLIS, G.B., DOBSON, J.E. "The Onset of Slugging in Horizontal Stratified Air-Water Flow", Int. J. Multiphase Flow, vol. 1, pp. 173-193, 1973.

(16) KORDYBAN, E.S., RANOV, T., "Mechanisms of Slug Formation in Horizontal Two-Phase Flow, J. of Basic Eng., Vol. 92, pp. 857-864, 1970.

(17) JEFFREYS, J. "On the Formation of Water Waves by Wind", Proc. Royal Soc., A107, 173-193, 1925.

(18) BENJAMIN, T.B., "Shearing Flow Over a Wavy Boundary", J. Fluid Mech., vol. 6, pp. 161-205, 1959.

(19) HANRATTY, T.J., ENGEN, J.M. , "Interaction Between a Turbulent Air Stream and a Moving Water Surface", AIChE.J., Vol. 3, pp. 299-304, 1957.

(20) FULFORD, G.D., "The Flow of Liquids in Thin Films", Advan. Chem. Eng., vol. 5, pp. 151-236, 1964.

(21) BROCK, R.R., "Periodic Permanent Roll Waves", Proc. ASCE, vol. 90, HYD 12, pp. 2565-2580, 1970.

(22) CHU, K.T., "Statistical Characteristics and Modelling of Wavy Liquid Films in Vertical Two-Phase Flow", PhD. Thesis, Univ. Houston, Tex., 1973.

(23) CHANG, J.S., GIRARD, R., RAMAN, AND TRAN, F.B.P., "Measurement of Void Fraction in Vertical Gas-Liquid Two-Phase Flow by Ring Type Capacitance Transducers", Mass Flow Measurement, T.R. HEDRICK and R.M. REIMER, Ed., ASME Press, New York, FED-17, Vol. 1, pp. 93-100, 1984.

(24) BARNEA, D., LUNINSKI, Y. AND TAITEL, Y., "Flow Regime Patterns in Horizontal and Vertical Two-Phase Flow in Small Diameter Pipes", Can. J. Chem. Eng., Vol. 61, pp. 617-620, 1983.

(25) NICHOLSON, M.K., NICKERSON, J.R., AZIZ, K. AND GREGORY, G.A., "A Comparison of Flow Regime and Pressure Drop in Adiabatic and Diabatic Two-Phase Flow Simulations", Proc. 7th Int. Conf. Heat Transfer, Munich, Paper No. TF11, Sept. 6-10.

NOMENCLATURE

A_ℓ, A'_ℓ = liquid-phase areas for pipe and annulus, respectively.

A_g, A'_g = gas-phase areas for pipe and annulus, respectively.

C_ℓ, C_g = friction factor coefficient for the liquid and gas, respectively.

d = diameter of annulus rod

D = inside diameter of tubeshell

D_ℓ, D_g = hydraulic diameters of liquid and gas-phases, respectively.

f_i = interfacial friction factor.

f_ℓ, f_g = gas and liquid phase friction factor, respectively.

F_B = buoyancy force defined by Eq. 33.

F_T = turbulent force defined by Eq. 34.

g = gravity.

h_ℓ, h_g = equilibrium liquid and gas levels, respectively.

r = radius coordinate of annulus rod.

S_ℓ, S'_ℓ = liquid-phase perimeters for pipe and annulus, respectively.

S_g, S'_g = gas-phase perimeter for pipe and annulus, respectively.

S_i, S'_i = gas-liquid interface length.

u_ℓ, u_g = liquid and gas phase velocities.

$U_{\ell s}, U_{gs}$ = superficial liquid and gas-phase velocities.

x_ℓ, x_g = liquid and gas phase friction-factor exponents.

Greek Letters

θ = angle.

γ = function defined by Eq. 12.

β = function defined by Eq. 22.

μ = viscosity.